Ab initio potential-energy curves and radial and rotational couplings for the process $N^{5+} + He \rightarrow N^{4+} + He^+$

Marie-Christine Bacchus-Montabonel

Laboratoire de Spectrométrie Ionique et Moléculaire, Université Lyon I, Campus de la Doua, Bâtiment 205, F-69622 Villeurbanne Cedex, France

Potential-energy curves of six $^1\Sigma^+$, two $^1\Pi$, and one $^1\Delta$ states have been determined for the $N^{5+} + He \rightarrow N^{4+} + He^+$ process by means of *ab initio* calculations with configuration interaction. The matrix elements of the operator d/dR between the four $^1\Sigma^+$ states and the two $^1\Pi$ states involved in the collisional process have been calculated by the rigorous finite-difference technique. A very peaked radial coupling matrix element is observed at 8.30 a.u. corresponding to an avoided crossing between the entry channel and the $^1\Sigma^+$ state dissociating to $\{N^{4+}(3d) + He^+\}$. Two other avoided crossings between $^1\Sigma^+$ states are observable at 7.50 and 6.35 a.u. Rotational and radial couplings involving $^1\Pi$ states have also been determined.

I. INTRODUCTION

Electron capture by multiply-charged ions from neutral atoms is of considerable interest in astrophysics and plasma fusion research and has been extensively studied both experimentally and theoretically.[1-3] Nevertheless up to now very few *ab initio* calculations are available[4,5] and most of the results are obtained by means of model potential methods.[6-8]

We report in this paper accurate *ab initio* results for potential-energy curves, radial and rotational matrix elements of the NHe^{5+} system. To the best of our knowledge, such *ab initio* results have not been published previously. This work has been undertaken in connection with the experimental investigations regarding the electron capture for the reactions

$$N^{5+}(^1S) + He(^1S) \rightarrow N^{4+} + He^+ \text{ or } N^{3+} + He^{2+}$$
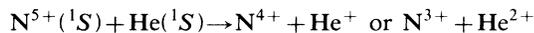
at collision energy about 50 keV.[3,9] These experiments have shown a quite different behavior for N^{5+} than for other multicharged ions such as the isoelectronic ion O^{6+}.[10] The single-electron-capture process has been shown to be predominant on the $n = 3$ level. A high probability of double capture has also been observed characterized by an intense peak corresponding to the $2s^2 \rightarrow 2s2p$ transition. These results are in agreement with the experimental data of Crandall[11] and Dijkkamp *et al.*[12]

In the first step of our theoretical investigation of the collisional process $N^{5+}(^1S) + He(^1S)$ we have considered only the single electron capture reaction. As this process has been shown experimentally to be predominant on the $n = 3$ level,[9] we have determined the potential energy curves for the entry channel $^1\Sigma^+\{N^{5+}(^1S) + He(^1S)\}$ and all the $^1\Sigma^+$ states corresponding to the $\{N^{4+}(1s^2, nl) + He^+(1s)\}$ configuration for $n = 2, 3$. We have also calculated the potential energy curves for the $^1\Pi$ and $^1\Delta$ states corresponding to the $\{N^{4+}(1s^2, 3l) + He^+(1s)\}$ configuration. All these calculations have been performed from an *ab initio* method including configuration interaction.[13]

The electron-capture processes are driven by nonadiabatic couplings between the molecular states. The radial coupling matrix elements $g_{KL}(R) = \langle \psi_K \mid \partial/\partial R \mid \psi_L \rangle$ which are large in region of avoided crossings have been calculated from the finite difference technique for all the pairs of states of a given symmetry ($^1\Sigma^+, ^1\Pi$) corresponding to the entry channel and to the configuration $\{N^{4+}(1s^2, 3l) + He^+(1s)\}$. We have also calculated the rotational coupling matrix elements for the $^1\Sigma^+$ and $^1\Pi$ states.

II. COMPUTATIONAL METHOD

The potential energy curves have been determined by *ab initio* calculations with configuration interaction for a large number of interatomic distances in the range $2.0 \leq R \leq 25.0$ a.u. The self-consistent-field (SCF) calculations have been performed by means of the PSHONDO program (a version of the HONDO program[14] modified by Daudey[15]) for the electronic configuration $(1\sigma)^2(2\sigma)^2$. The configuration interaction (CI) has been performed according to the configuration interaction by perturbation of a multiconfiguration wave function selected iteratively (CIPSI) method.[13] For the $^1\Sigma^+$ states, 138 determinants have been involved in the CI space with a threshold $\eta = 0.01$ for the perturbation contribution to the wave function while 124 determinants have been used for the $^1\Pi$ states and 24 for the $^1\Delta$ state. A larger number of configurations are then taken into account by means of the perturbation procedure (609 efficient states have been generated in the calculation of $^1\Sigma^+$ states and 362 for $^1\Pi$ states). According to the deep energy difference between 1σ and 2σ, the 1σ orbital has been frozen in the CI procedure.

The basis of atomic functions used in the calculation is a $9s5p3d$ basis of Gaussian functions for nitrogen and a $4s1p$ basis for helium. It has been optimized from the $6.311G^*$ basis of Krishnan *et al.*[16] For nitrogen, two diffuse s functions have been added to represent the $3s$ and $4s$ orbitals and two p functions have been added for the description of the $3p$ and $4p$ levels. One diffuse d

TABLE I. Basis of atomic orbitals.

	N		He	
	Exponent	Coefficient	Exponent	Coefficient
s	6670.946 946	0.000 276	97.708 827	0.007 588
	965.269 671	0.002 199	14.857 311	0.054 135
	225.703 810	0.010 237	3.373 390	0.215 948
	71.707 703	0.031 217	0.896 865	1.0
	15.106 097	0.084 000	0.250 773	1.0
	29.107 097	1.0	0.74	1.0
	7.597 890	1.0		
	3.459 844	1.0		
	1.355 819	1.0		
	0.610 993	1.0		
	0.273 544	1.0		
	0.13	1.0		
	0.057	1.0		
p	32.870 575	0.019 366	0.27	1.0
	7.451 735	0.131 861		
	2.557 111	0.394 529		
	1.059 492	1.0		
	0.497 407	1.0		
	0.133	1.0		
	0.05	1.0		
d	0.732	1.0		
	0.203 805	1.0		
	0.04	1.0		

function represents the $4d$ orbital. The optimization has been performed at the SCF level on $N^{3+}(2s^2), N^{3+}(2s2p)$, and $N^{3+}(2p3d)$ for nitrogen center and on $He(1s^2)$ for helium. The diffuse functions cannot be optimized with the monoconfiguration SCF procedure we have used, so

TABLE II. Comparison of calculated atomic levels with experimental data [Bashkin and Stoner (Ref. 17)] (in a.u.).

	Experiment (a.u.)	CIPSI calculation (a.u.)
$N^{5+}(1s^2)$	175.39	174.87
$N^{4+}(3d)$	137.55	137.65
$N^{4+}(3p)$	136.73	136.65
$N^{4+}(3s)$	134.04	133.32
$N^{4+}(2p)$	87.47	86.76
$N^{4+}(2s)$	77.48	76.75
$N^{3+}(2s4d)$	63.82	64.36
$N^{3+}(2s4p)$	62.87	62.99
$N^{3+}(2s4s)$	61.39	61.46
$N^{3+}(2s3d)$	53.22	53.63
$N^{3+}(2s3p)$	50.16	50.27
$N^{3+}(2s3s)$	48.22	48.17
$N^{3+}(2p2p)$	29.19	29.81
$N^{3+}(2s2p)$	16.21	16.85
$N^{3+}(2s^2)$	0	0
$He^+(2p)$	65.41	68.57
$He^+(2s)$	65.41	66.51
$He^+(1s)$	24.59	23.88
$He(1s^2)$	0	0

they have been optimized directly at the CI level on $N^{4+}(3s)$, $N^{3+}(2s4s)$, $N^{4+}(3p)$, $N^{3+}(2s4p)$, and $N^{3+}(2s4d)$ for nitrogen and on $He^+(2s)$ and $He^{2+}(2p)$ for helium. The exponents and contraction coefficients are given in Table I.

A fairly reasonable agreement with experiment[17] is obtained for a large number of atomic levels of nitrogen (Table II). The discrepancy is never more than 0.73 eV and is often about 0.08 eV. The agreement is a little less good for He^+ excited states, especially $He^+(2p)$ (Table II), but these states are energetically too high to be involved in this collisional process.

The evaluation of the radial coupling matrix elements between molecular states of a same symmetry $g_{KL}(R) = \langle \psi_K \mid \partial/\partial R \mid \psi_L \rangle$ has been performed by the finite difference technique[18−21]

$$g_{KL}(R) = \lim_{\Delta \to 0} \Delta^{-1} \langle \psi_K(R) \mid \psi_L(R+\Delta) \rangle . \qquad (1)$$

g_{KL} breaks up into two terms

$$g_{KL} = g_{KL}^{MO} + g_{KL}^{CI}$$

involving, respectively, the differentiation of the molecular orbitals (g_{KL}^{MO}) and of the CI coefficients (g_{KL}^{CI}),

$$g_{KL}^{MO} = \sum_{i,j} \rho_{ij}^{KL} \left\langle \phi_i \left| \frac{\partial}{\partial R} \right| \phi_j \right\rangle$$

and

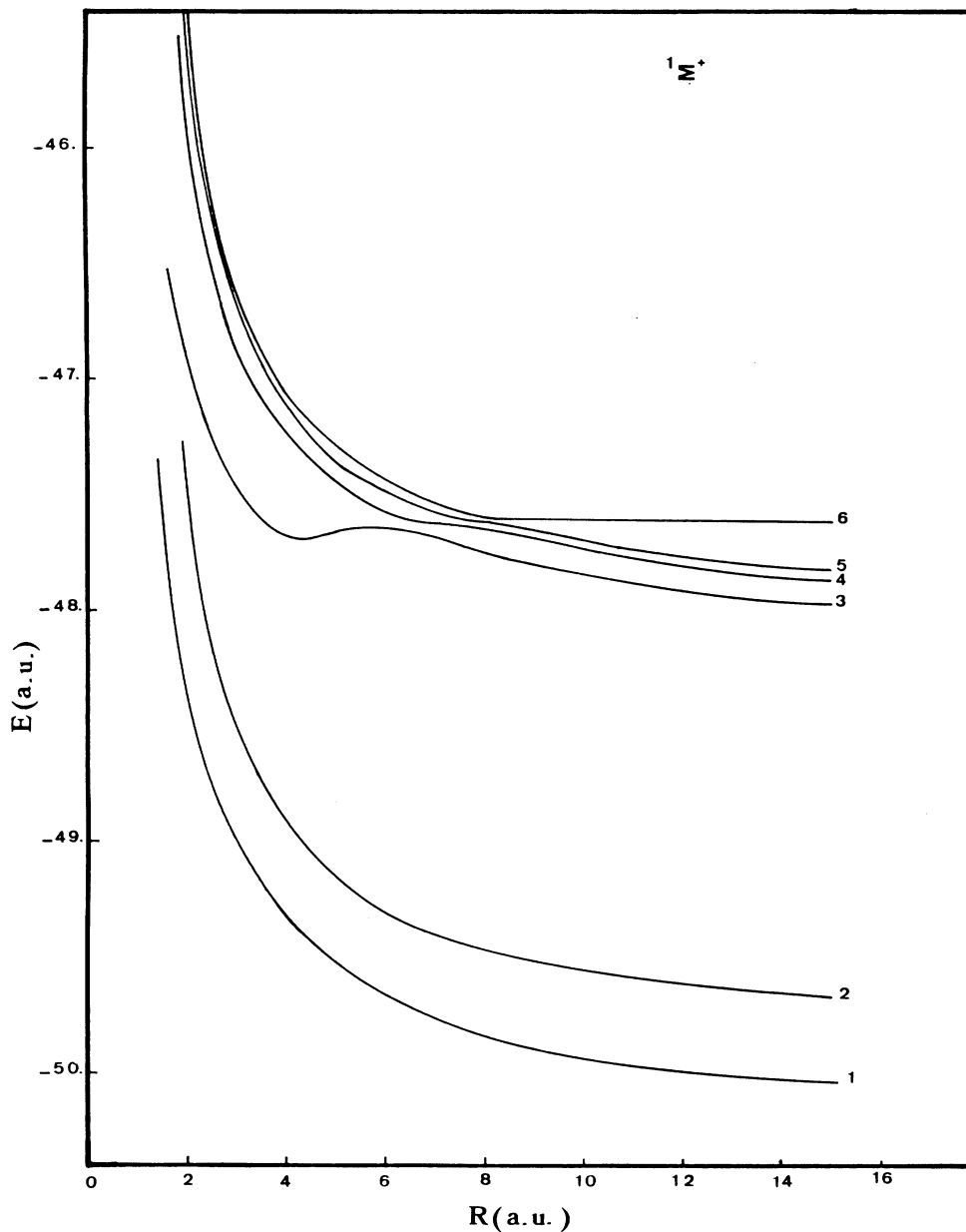$$g_{KL}^{CI} = C_K^+ \frac{\partial C_L}{\partial R} ,$$

FIG. 1. Potential energy curves of six $^1\Sigma^+$ states of NHe^{5+}. 1, state dissociating to $\{N^{4+}(2s)+He^+(1s)\}$; 2, state dissociating to $\{N^{4+}(2p)+He^+(1s)\}$; 3, state dissociating to $\{N^{4+}(3s)+He^+(1s)\}$; 4, state dissociating to $\{N^{4+}(3p)+He^+(1s)\}$; 5, state dissociating to $\{N^{4+}(3d)+He^+(1s)\}$; 6, state dissociating to $\{N^{5+}(1s^2)+He^+(1s^2)\}$.

where $\{\phi_i\}$ designates the molecular-orbital set, ρ^{KL} the one-particle transition density matrix, and C_K the Kth CI eigenvector (the labeling of states K,L is displayed in Fig. 1). For the parameter Δ in Eq. (1), we have chosen $\Delta = 0.0012$ a.u. The rotational coupling matrix elements defined by $\langle \psi_K \mid iLy \mid \psi_L \rangle$ have been easily evaluated analytically by use of the L_+ and L_- operators.

III. RESULTS

Calculated values of the energy of the six $^1\Sigma^+$ states investigated are given in Table III for various values of R

from 2 to 25 a.u. The corresponding potential energy curves are shown in Fig. 1. Similar results are reported in Table IV and in Fig. 2 for $^1\Pi$ and $^1\Delta$ states in the range 5.0 a.u. $\leq R \leq 18$ a.u. The asymptotic values of the energy are seen to be in quite good agreement with experiment.[17] For the $^1\Sigma^+$ states the values obtained from the configuration interaction performed at 25 a.u. corrected for the Coulombic repulsion term at this distance are reported in Table V and show differences with experimental data between 0.08 and 0.38 eV over a range of 74 eV. For $^1\Pi$ states, the energy difference between the two states (evaluated from the CI results at 18 a.u.) is of 1.035 eV to

AB INITIO POTENTIAL-ENERGY CURVES AND RADIAL AND . . .

TABLE III. Variation with R of the potential energy for six $^1\Sigma^+$ states of NHe^{5+} (in a.u.).

R (a.u.)	E_1 (a.u.)	E_2 (a.u.)	E_3 (a.u.)	E_4 (a.u.)	E_5 (a.u.)	E_6 (a.u.)
2.0	−48.297 476	−47.499 517	−46.901 027	−45.840 542	−45.515 900	−45.307 579
4.0	−49.330 620	−48.962 526	−47.682 905	−47.222 029	−47.093 975	−47.069 280
5.0	−49.525 163	−49.156 014	−47.661 223	−47.446 209	−47.367 130	−47.282 185
5.5	−49.596 474	−49.227 162	−47.650 425	−47.522 966	−47.419 629	−47.359 390
6.0	−49.656 178	−49.286 752	−47.644 384	−47.581 400	−47.482 694	−47.423 470
6.25	−49.682 516	−49.313 040	−47.645 867	−47.602 722	−47.509 649	−47.451 271
6.5	−49.706 866	−49.337 343	−47.654 222	−47.615 010	−47.534 147	−47.476 991
6.75	−49.729 437	−49.359 869	−47.669 491	−47.619 096	−47.556 428	−47.500 457
7.0	−49.750 417	−49.380 808	−47.687 087	−47.619 961	−47.576 809	−47.522 847
7.25	−49.769 967	−49.400 319	−47.704 680	−47.620 271	−47.595 195	−47.543 229
7.5	−49.788 226	−49.418 540	−47.721 602	−47.622 772	−47.609 775	−47.562 448
7.75	−49.805 319	−49.435 598	−47.737 685	−47.633 466	−47.614 712	−47.579 946
8.0	−49.821 352	−49.451 599	−47.752 919	−47.647 735	−47.615 663	−47.596 519
8.25	−49.836 421	−49.466 638	−47.767 335	−47.661 835	−47.615 245	−47.611 941
8.5	−49.850 611	−49.480 800	−47.780 975	−47.675 294	−47.626 807	−47.614 564
8.75	−49.863 995	−49.494 158	−47.793 897	−47.688 060	−47.640 529	−47.614 253
9.0	−49.876 641	−49.506 780	−47.806 148	−47.700 168	−47.676 329	−47.613 945
10.0	−49.920 935	−49.550 999	−47.849 342	−47.742 835	−47.698 722	−47.612 980
13.0	−50.013 064	−49.642 990	−47.940 172	−47.832 613	−47.791 989	−47.611 797
15.0	−50.054 050	−49.683 930	−47.980 864	−47.872 932	−47.833 213	−47.611 533
18.0	−50.098 467	−49.728 308	−48.025 089	−47.916 844	−47.877 766	−47.611 366
25.0	−50.160 671	−49.790 477	−48.087 165	−47.978 637	−47.940 025	−47.611 254

TABLE IV. Variation with R of the potential energy for two $^1\Pi$ and one $^1\Delta$ states of NHe^{5+} (in a.u.). (Labels are defined in Fig. 2.)

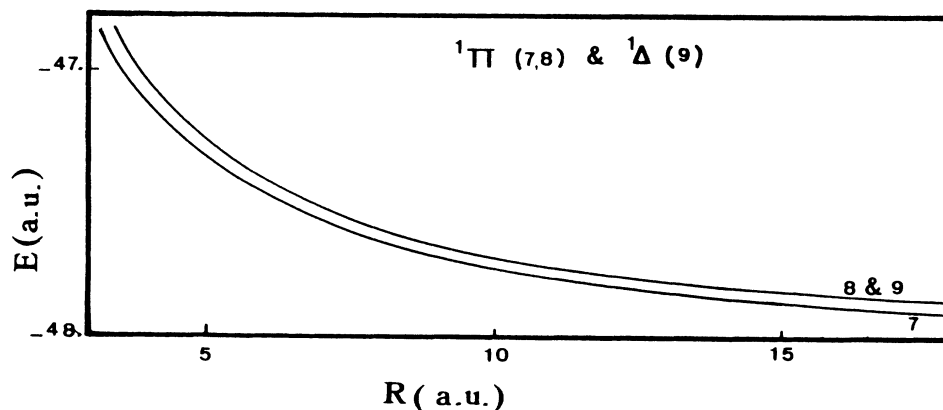| R (a.u.)	$^1\Pi$		$^1\Delta$
	E_7 (a.u.)	E_8 (a.u.)	E_9 (a.u.)
5.0	−47.352 479	−47.283 987	−47.291 637
6.0	−47.479 581	−47.424 212	−47.427 933
6.35	−47.514 848	−47.462 442	
7.0	−47.571 283	−47.523 129	−47.524 965
7.5	−47.608 240	−47.562 449	
8.0	−47.640 724	−47.596 701	−47.597 481
8.30	−47.658 391	−47.615 215	
9.0	−47.695 156	−47.653 500	−47.653 727
10.0	−47.738 955	−47.698 669	−47.698 634
13.0	−47.830 512	−47.791 898	
15.0	−47.871 393	−47.833 131	−47.832 905
18.0	−47.915 762	−47.877 702	

FIG. 2. Potential energy curves of two $^1\Pi$ states and one $^1\Delta$ state of NHe^{5+}. ———, $^1\Pi$ states; 7, state dissociating to $\{N^{4+}(3p)+He^+(1s)\}$; 8, state dissociating to $\{N^{4+}(3d)+He^+(1s)\}$. – – –, $^1\Delta$ state (9) dissociating to $\{N^{4+}(3d)+He^+(1s)\}$. It is nearly superposed to the second $^1\Pi$ state (8).

TABLE V. Comparison of experimental data (Ref. 17) with theoretical energies of $^1\Sigma^+$ states obtained by a CIPSI calculation at 25 a.u. corrected by the Coulombic repulsion term. (Labels 1 to 6 are defined in Fig. 1.)

	Theoretical energies (eV)	Experimental energies (eV)
E_1	0	0
E_2	10.069	9.993
E_3	56.399	56.560
E_4	59.351	59.247
E_5	60.401	60.068
E_6	73.696	73.312

TABLE VI. Variation with R of the radial nonadiabatic couplings $g_{KL}(R)$, $K,L = \{3,4,5,6\}$ for $^1\Sigma^+$ states and $g'_{KL}(R)$, $K,L = \{7,8\}$ for $^1\Pi$ states (in a.u.).

R (a.u.)	g_{34} (a.u.)	g_{35} (a.u.)	g_{36} (a.u.)	g_{45} (a.u.)	g_{46} (a.u.)	g_{56} (a.u.)	g'_{78} (a.u.)
5.0	−0.252 873	0.131 924	−0.046 527	0.146 508	0.050 553	0.098 422	
5.5						0.062 046	
6.0	−0.667 263	0.094 756	−0.037 158	0.032 383	0.011 890	0.102 617	0.081 902
6.25	−1.157 025						
6.35	−1.228 055	0.073 937	−0.014 802	−0.058 701	0.024 565	0.092 241	0.092 836
6.5	−1.163 18	0.090 663	0.026 863	−0.063 227	0.035 507	0.080 315	
6.75	−0.666 422			−0.144 866			
7.0	−0.296 766	−0.062 533	0.007 164	−0.246 225	0.038 361	0.066 106	0.080 634
7.25	−0.217 261			−0.870 159			
7.5	−0.137 930	0.043 356	0.008 682	−2.528 518	−0.062 229	−0.016 731	0.069 908
7.75	−0.097 472			−1.146 693			
8.0	−0.085 951	−0.027 557	−0.018 637	−0.348 678	−0.043 326	−0.113 795	0.055 306
8.15						−0.915 538	
8.20						−1.872 673	
8.25	−0.095 545			−0.158 514		−8.140 281	
8.30	−0.090 221	−0.012 691	−0.005 302	−0.144 454	−0.058 497	−12.213 971	0.056 773
8.32						−6.180 302	
8.35						−2.628 724	
8.5	−0.080 977	−0.006 524	0.002 331	0.068 675	−0.093 405	−0.236 216	
8.75	−0.084 113	−0.010 760		0.072 692		−0.050 762	
9.0	−0.074 428	−0.075 367	0.007 028	−0.353 767	0.054 075	−0.033 376	0.107 546
10.0	−0.049 260	−0.002 554	0.000 270	0.063 194	−0.006 403	0.007 722	
13.0	−0.039 255	−0.002 658	−0.000 526	0.019 168	0.003 116	0.007 889	
15.0	−0.031 116	−0.001 985	−0.001 164	−0.034 544	−0.000 352	0.003 196	

TABLE VII. Rotational coupling matrix elements between $^1\Sigma^+$ (labeled 3,4,5,6) and $^1\Pi$ (labeled 7,8) states of NHe^{5+} (in a.u.) (for the labels see captions of Figs. 1 and 2).

| R (a.u.)	g_{73}^{rot}	g_{74}^{rot}	g_{75}^{rot}	g_{76}^{rot}	g_{83}^{rot}	g_{84}^{rot}	g_{85}^{rot}	g_{86}^{rot}
5	0.597	0.198	0.753	−0.400	−0.161	0.115	0.209	1.484
6	0.460	0.154	1.078	−0.327	−0.124	0.066	0.293	1.540
7	0.335	0.279	1.048	−0.272	−0.039	−0.139	0.271	1.594
8	0.237	1.064	0.107	−0.229	−0.023	−0.276	−0.086	1.632
9	0.181	1.052	0.157	−0.017	−0.018	−0.237	−1.374	−0.018
10	0.143	1.038	0.159	−0.003	−0.014	−0.204	−1.684	−0.002
13	0.081	1.016	0.099	0.0	−0.008	−0.132	−1.714	0.0
15	0.060	1.008	0.076	0.0	−0.006	−0.101	−1.722	0.0
18	0.041	1.004	0.053	0.0	−0.004	−0.071	−1.726	0.0
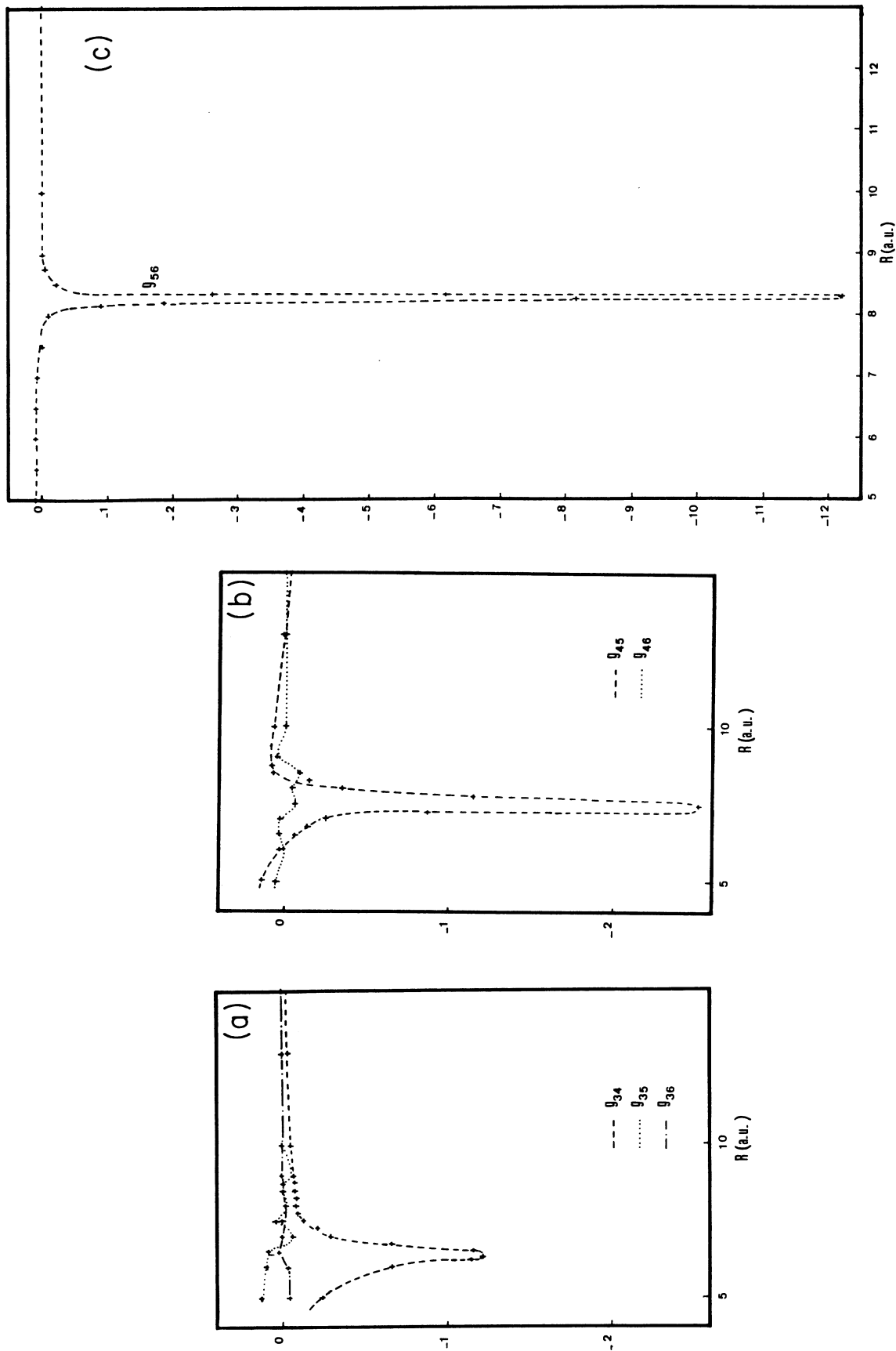
FIG. 3. (a) Nonadiabatic radial coupling matrix elements g_{34}, g_{35}, g_{36} calculated by the finite difference technique for $^1\Sigma^+$ states. (b) Nonadiabatic radial coupling matrix elements g_{45}, g_{46} calculated by the finite difference technique for $^1\Sigma^+$ states. (c) Nonadiabatic radial coupling matrix element g_{56} calculated by the finite difference technique for $^1\Sigma^+$ states.
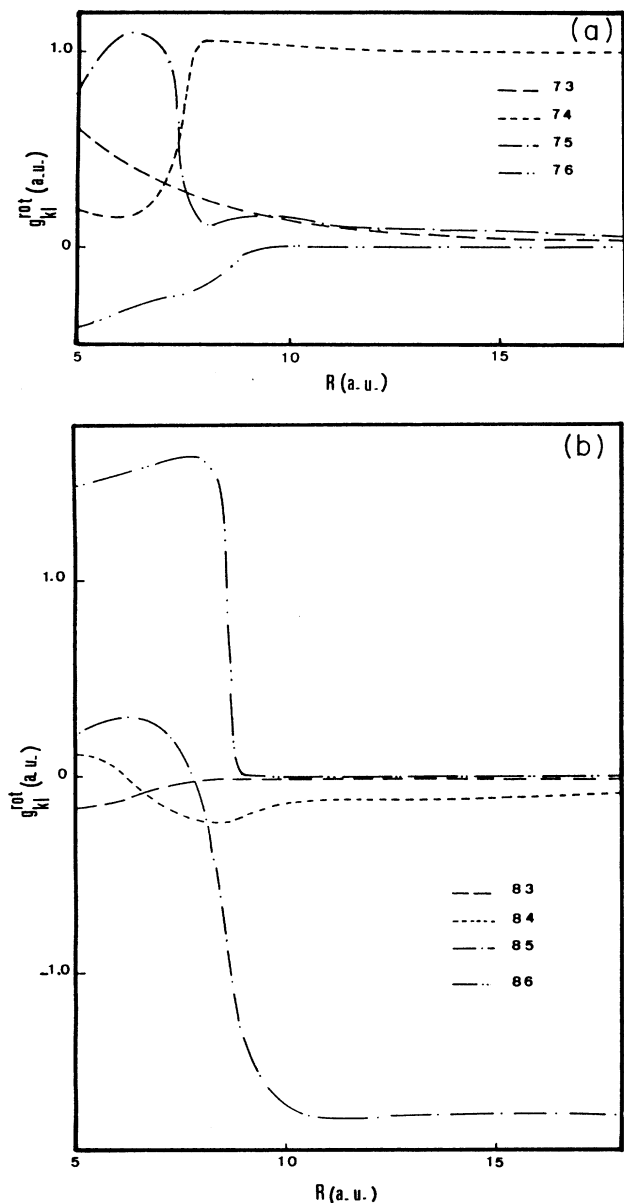
FIG. 4. (a) Rotational coupling matrix elements between $^1\Sigma^+$ (labeled 3,4,5,6) and $^1\Pi$ (labeled 7) states of NHe^{5+}. (b) Rotational coupling matrix elements between $^1\Sigma^+$ (labeled 3,4,5,6) and $^1\Pi$ (labeled 8) states of NHe^{5+}.

The potential-energy curves for the $^1\Sigma^+$ states show three avoided crossings in the range 6 a.u. $\leq R \leq 9$ a.u., between the entry channel and the three states corresponding to the configuration $\{N^{4+}(1s^2,3l)+He^+(1s)\}$. In correspondence with these avoided crossings between the $^1\Sigma^+$ states the g_{34}, g_{45}, and g_{56} functions present a sharp peak, respectively, at 6.35, 7.50, and 8.30 a.u. These peaks are approximately 1.23, 2.53, and 12.21 a.u. high, respectively, and 0.75, 0.50, and less than 0.10 a.u. wide at half height. The other matrix elements g_{35}, g_{36}, and g_{46} are largely smaller and show only small variations due partially to the precision of the calculation. The radial coupling matrix elements between $^1\Pi$ states evaluated in the interacting internuclear region (6 a.u. $\leq R \leq 9$ a.u.) are small and present also very smooth variations.

In order to complete the nonadiabatic coupling matrix we have also calculated the rotational coupling matrix elements between the two $^1\Pi$ and the four $^1\Sigma^+$ states (including the entry channel) involved in the collisional process. The calculated values are displayed in Table VII and shown in Fig. 4. At large internuclear distances, rotational couplings are seen to be rather large for $^1\Pi$ and $^1\Sigma^+$ states corresponding to the same configuration, i.e., g_{74}^{rot} for the $\{N^{4+}(3p)+He^+(1s)\}$ configuration and g_{85}^{rot} for the $\{N^{4+}(3d)+He^+(1s)\}$ configuration.

IV. CONCLUSION

This work provides for the first time, to the best of our knowledge, accurate *ab initio* potential-energy curves, and radial and rotational couplings for the $^1\Sigma^+$, $^1\Pi$, and $^1\Delta$ states of the system NHe^{5+} involved in the single-electron-capture process $N^{5+}(1s^2)+He(1s^2) \rightarrow N^{4+}(1s^2,3l)+He^+(1s)$.

The configuration-interaction method used here (CIPSI algorithm) for the system NHe^{5+} provides the same rate of accuracy as the spin-coupled valence-bond method previously used for the system CH^{3+}.[4] Such *ab initio* methods could provide significant improvements in understanding of the charge transfer in multicharged ions collisions. The method used in this work could be extended to charge exchange involving metastable ions as $N^{5+}(1s2s)$ which would be of great interest in the actual development of multicharged ions with neutral species reactions.

be compared to the experimental value of 0.819 eV.

The calculated values for the nonadiabatic radial couplings are presented in Table VI for all the pairs of states: entry channel, $^1\Sigma^+$ and $^1\Pi$ states dissociating to $\{N^{4+}(1s^2,3l)+He^+(1s)\}$. For $^1\Sigma^+$ states, radial coupling matrix elements are shown in Figs. 3(a)–3(c).

[1]S. Bliman, D. Hitz, B. Jacquot, C. Harel, and A. Salin, J. Phys. B **16**, 2849 (1983).

[2]A. Bordenave-Montesquieu, P. Benoît-Cattin, A. Gleizes, S. Dousson, and D. Hitz, J. Phys. B **18**, L195 (1985).

[3]P. H. Cotte, M. Druetta, S. Martin, A. Denis, J. Désesquelles, D. Hitz and S. Dousson, Nucl. Instrum. Methods Phys. Res. B **9**, 403 (1985).

[4]D. L. Cooper, M. J. Ford, J. Gerratt, and M. Raimondi, Phys.

Rev. A **34**, 1752 (1986).

[5]M. Kimura and R. E. Olson, Phys. Rev. A **31**, 489 (1985); J. Phys. B **18**, 2729 (1985).

[6]M. Gargaud, J. Hanssen, R. McCarroll, and P. Valiron, J. Phys. B **14**, 2259 (1981).

[7]M. Gargaud and R. McCarroll, J. Phys. B **18**, 463 (1985).

[8]J. Hansen, R. Gayet, C. Harel, and A. Salin, J. Phys. B **17**, L323 (1984).

[9]P. H. Cotte, doctorate thesis, University of Lyon, France, 1984.

[10]Y. S. Gordeev, D. Dijkkamp, A. G. Drentje, and F. J. De Heer, Phys. Rev. Lett. **50**, 1842 (1983).

[11]D. H. Crandall, Phys. Rev. A **16**, 958 (1977).

[12]D. Dijkkamp, D. Ciric, E. Vlieg, A. De Boer, and F. J. De Heer, J. Phys. B **18**, 4763 (1985).

[13]B. Huron, J. P. Malrieu, and P. Rancurel, J. Chem. Phys. **58**, 5745 (1973).

[14]M. Dupuis, J. Rys, and H. F. King, HONDO 76, Q.C.P.E. Program No. 338 (1976).

[15]J. P. Daudey (unpublished).

[16]R. Krishnan, J. S. Binkley, R. Seeger, and J. A. Pople, J. Chem. Phys. **72**, 650 (1980).

[17]S. Bashkin and J. O. Stoner, *Atomic Energy Levels and Grotrian Diagrams* (North-Holland, Amsterdam, 1975).

[18]C. Galloy and J. C. Lorquet, J. Chem. Phys. **67**, 4672 (1977).

[19]R. Cimiraglia, T. K. Ha, R. Meyer, and H. N. Günthard, Chem. Phys. **66**, 209 (1982).

[20]M. Persico and V. Bonačić-Koutecký, J. Chem. Phys. **76**, 6018 (1982).

[21]M. C. Bacchus-Montabonel, R. Cimiraglia, and M. Persico, J. Phys. B **17**, 1931 (1984).